Supporting Information

Development of high refractive index UiO-66 framework derivatives via ligand halogenation

Marvin Treger[1,2], Adrian Hannebauer[1], Peter Behrens[1,2] and Andreas M. Schneider[1,2]

[1]Institute of Inorganic Chemistry, Leibniz University Hannover, Callinstr. 9, 30167 Hannover, Germany
[2]Cluster of Excellence PhoenixD (Photonics, Optics, and Engineering – Innovation Across Disciplines), Hannover, Germany

Table of Contents

Section 1 Experimental Details

Chemicals

Zirconium (IV) chloride (>99.5%, $ZrCl_4$, Sigma Aldrich), *N,N*-dimethylformamide (99.8%, DMF, Sigma Aldrich), formic acid (>98%, HCOOH, Merck), terephthalic acid (99%, $C_8H_6O_4$ (H_2BDC), Honeywell), 2-fluoroterephthalic acid (98%, $C_8H_5FO_4$ (H_2BDC-F), ABCR), 2-chloroterephthalic acid (98%, $C_8H_5ClO_4$ (H_2BDC-Cl), BLDpharm), 2-bromoterephthalic acid (97%, $C_8H_5BrO_4$ (H_2BDC-Br), ABCR), 2-iodoterephthalic acid (95%, $C_8H_5IO_4$ (H_2BDC-I), ABCR), 2,5-iodoterephthalic acid (98%, $C_8H_5I_2O_4$ (H_2BDC-I_2), AmBeed), Acetone (99.5 %, C_4H_6O Sigma Aldrich), Calcium chloride dehydrate (≥ 99 % , $CaCl_2 \cdot 2\ H_2O$, Sigma Aldrich), deuterated dimethyl sulfoxide for NMR analysis (≥ 99.8 % D, C_2H_6OS, Eurisotop), deuterated water for NMR analysis (99,98 % D, D_2O, Sigma Aldrich), Hydrofluoric acid (40 % in water, HF, Fisherscientific) were used without further purification.

Synthesis of MOFs

UiO-66

Nearly defect-free UiO-66 was synthesized according to Shearer *et al*., by sequentially adding 0.777 g $ZrCl_4$ (1 eq), 0.552 mL 37% HCl (2 eq) and 1.104 g H_2BDC (2 eq) to 20 mL DMF (77.5 eq) to a beaker.[1] After stirring this solution for 30 minutes a clear solution was obtained and transferred to a Teflon liner and sealed in a stainless-steel autoclave, which was heated at 220 °C for 20 h. The resulting white powder was separated via centrifugation, washed with DMF and acetone and dried under vacuum overnight. Afterwards the powder was purified using a Soxhlet-extraction with acetone for 24 h and activated at 150 °C for 20 h.

UiO-66-F

UiO-66-F was synthesized in a 100 mL Pyrex glass vessel by sequentially adding 0.1505 g $ZrCl_4$ (1 eq), 0.609 mL formic acid (25 eq) and 0.1189 g H_2BDC−F (1 eq) in 25 mL DMF (500 eq). The glass vessel was sealed and heated at 120 °C for 24 h. The resulting powder was separated via centrifugation, washed with DMF and acetone and dried under vacuum overnight. Afterwards the powder was purified using a Soxhlet-extraction with acetone for 24 h and activated at 120 °C for 20 h.

UiO-66-Cl

UiO-66-Cl was synthesized in a 100 mL Pyrex glass vessel by sequentially adding 0.1505 g $ZrCl_4$ (1 eq), 0.609 mL formic acid (25 eq) and 0.1295 g H_2BDC−Cl (1 eq) in 25 mL DMF (500 eq). The glass vessel was sealed and heated at 120 °C for 24 h. The resulting powder was separated via centrifugation, washed with DMF and acetone and dried under vacuum overnight. Afterwards the powder was purified using a Soxhlet-extraction with acetone for 24 h and activated at 120 °C for 20 h.

UiO-66-Br

UiO-66-Br was synthesized in a 100 mL Pyrex glass vessel by sequentially adding 0.1505 g $ZrCl_4$ (1 eq), 1.218 mL formic acid (50 eq) and 0.1582 g $H_2BDC{-}Br$ (1 eq) in 25 mL DMF (500 eq). The glass vessel was sealed and heated at 120 °C for 24 h. The resulting powder was separated via centrifugation, washed with DMF and acetone and dried under vacuum overnight. Afterwards the powder was purified using a Soxhlet-extraction with acetone for 24 h and activated at 120 °C for 20 h.

UiO-66-I

UiO-66-I was synthesized in a 100 mL Pyrex glass vessel by sequentially adding 0.1505 g $ZrCl_4$ (1 eq), 6.091 mL formic acid (250 eq) and 0.1886 g $H_2BDC{-}I$ (1 eq) in 25 mL DMF (500 eq). The glass vessel was sealed and heated at 120 °C for 24 h. The resulting powder was separated via centrifugation, washed with DMF and acetone and dried under vacuum overnight. Afterwards the powder was purified using a Soxhlet-extraction with acetone for 24 h and activated at 120 °C for 20 h.

UiO-66-I_2

UiO-66-I_2 was synthesized in a 100 mL Pyrex glass vessel by sequentially adding 0.1505 g $ZrCl_4$ (1 eq), 2.436 mL formic acid (100 eq) and 0.2669 g $H_2BDC{-}I_2$ (1 eq) in 25 mL DMF (500 eq). The glass vessel was sealed and heated at 120 °C for 24 h. The resulting powder was separated via centrifugation, washed with DMF and acetone and dried under vacuum overnight. Afterwards the powder was purified using a Soxhlet-extraction with acetone for 24 h and activated at 120 °C for 20 h.

Characterization of UiO-66-I_2

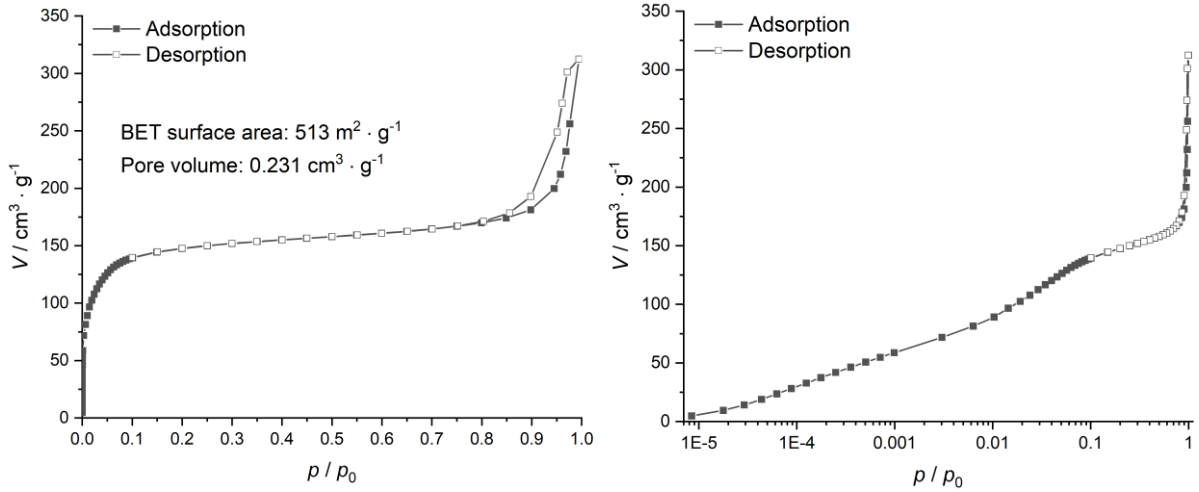

Figure S1. Ar sorption @ 87 K of UiO-66-I_2. The pore volume was evaluated at p/p_0 = 0.9.

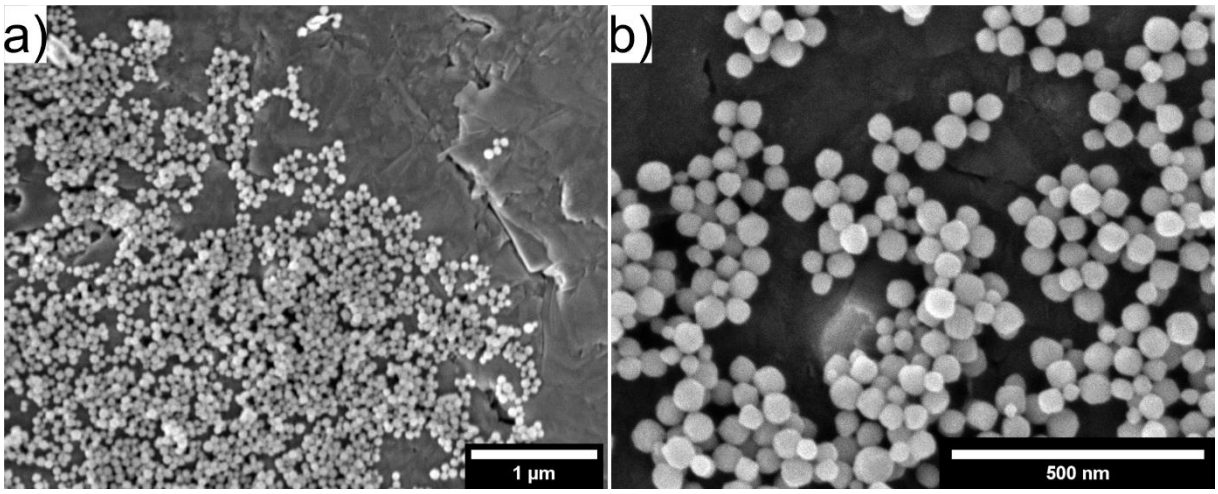

Figure S2. SEM images of UiO-66-I_2 with a magnification of a) 25000 and b) 100000 times.

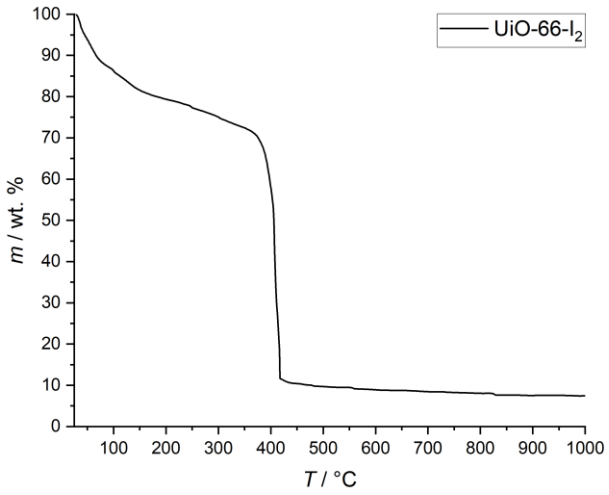

Figure S3. Thermogravimetric measurement of UiO-66-I_2.

NMR Spectra

The successful non-destructive incorporation of the linkers into the framework and the absence of guest molecules after washing and drying the powders were monitored with ^{1}H-NMR-spectroscopy on digested samples.

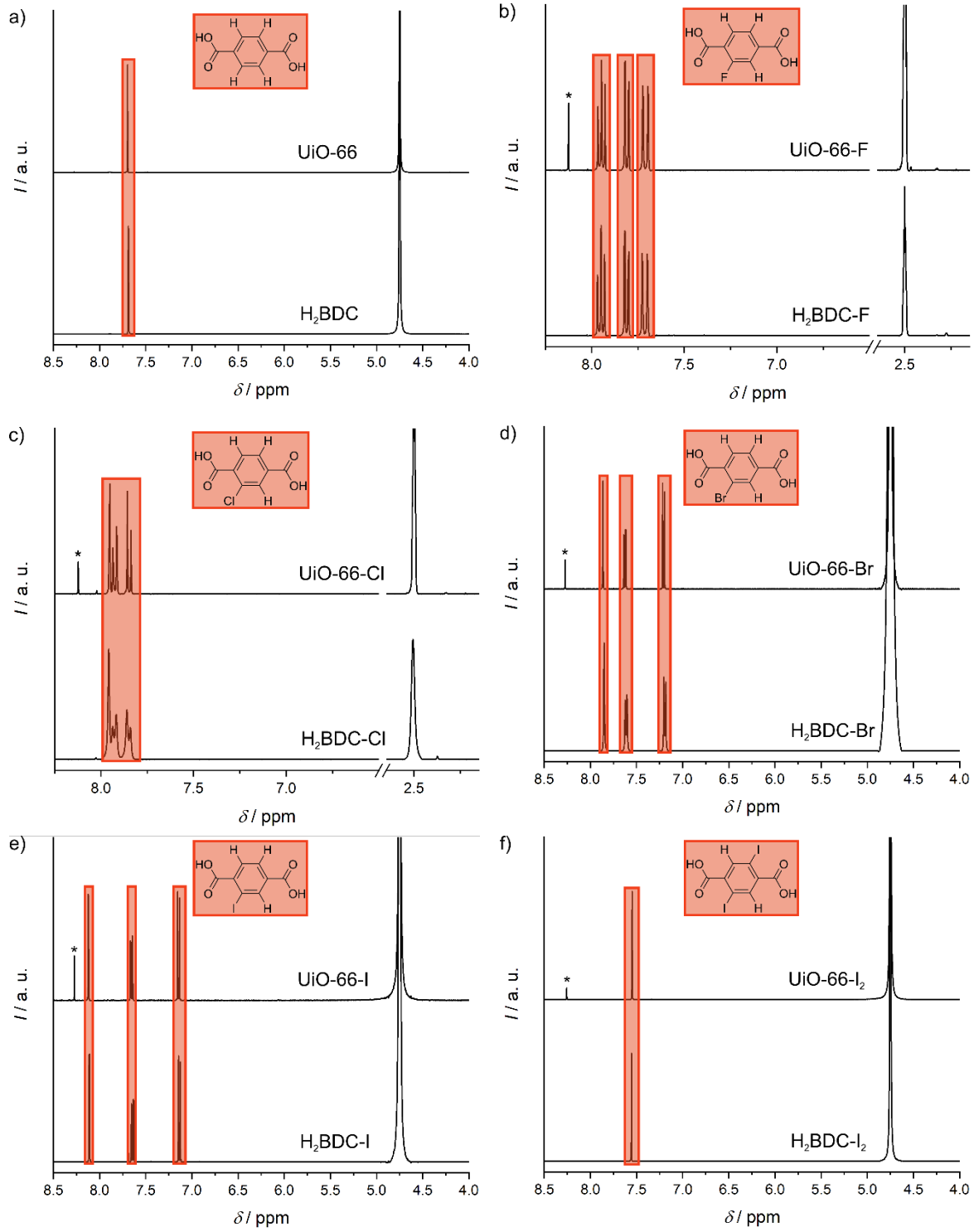

Figure S4. ^{1}H-NMR-Spectra of digested MOFs compared to the linker. a) UiO-66, b) UiO-66−F, c) UiO-66−Cl, d) UiO-66-Br, e) UiO-66-I, f) UiO-66-I_2. The * indicates the presents of formic acid, which is incorporated into the framework. Peaks at 2.5 and 4.75 ppm represent the NMR-solvent DMSO-d_6 and D_2O, respectively.

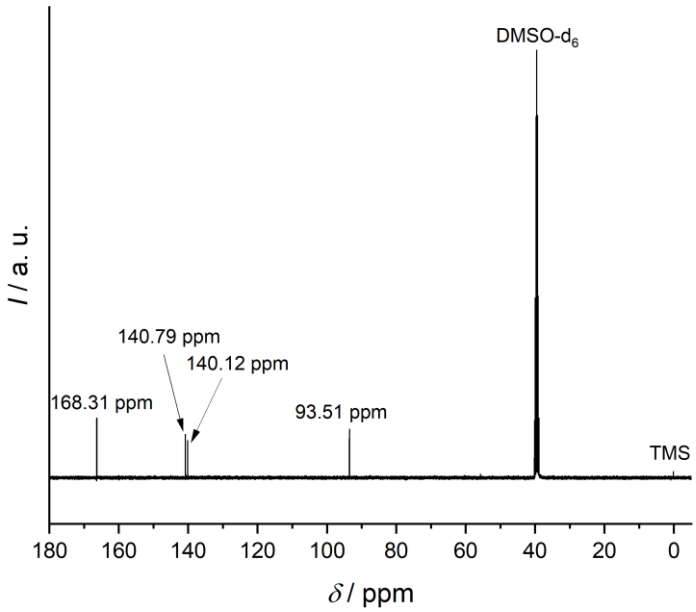

Figure S5. ^{13}C-NMR-Spectrum of 2,5-diiodo-1,4-dibenzoic acid. The presence of four signals underlines the *para* position of the iodine atoms and is in accordance with the literature values (92.99 ppm, 140.02 ppm, 140.66 ppm and 165.94 ppm).[2]

UV-Vis Spectra

To validate the electronic structure calculations, UV-Vis DRS was performed.

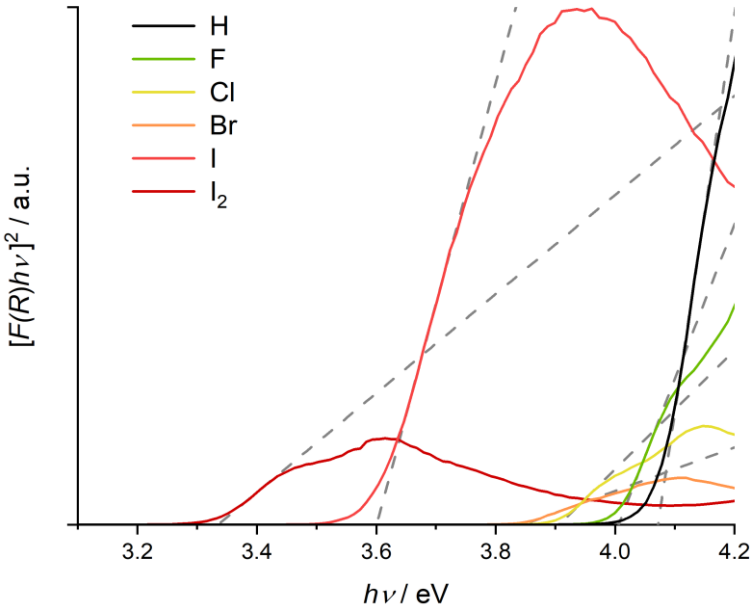

Figure S6. Tauc plot of recorded UV-Vis-Spectra.

Section 2 Plane wave basis set convergence

The kinetic plane wave energy cutoff convergence was tested with respect to the lattice parameter *a* of the primitive cells and the threshold was set to a change of 0.01 Å. The sampling of the Brillouin zone was tested with respect to the total energy and the lattice parameter *a* of the primitive cells. Analogous to the kinetic plane wave energy cutoff convergence, the threshold for the change of the lattice parameter was set to a change of 0.01 Å.

UiO-66

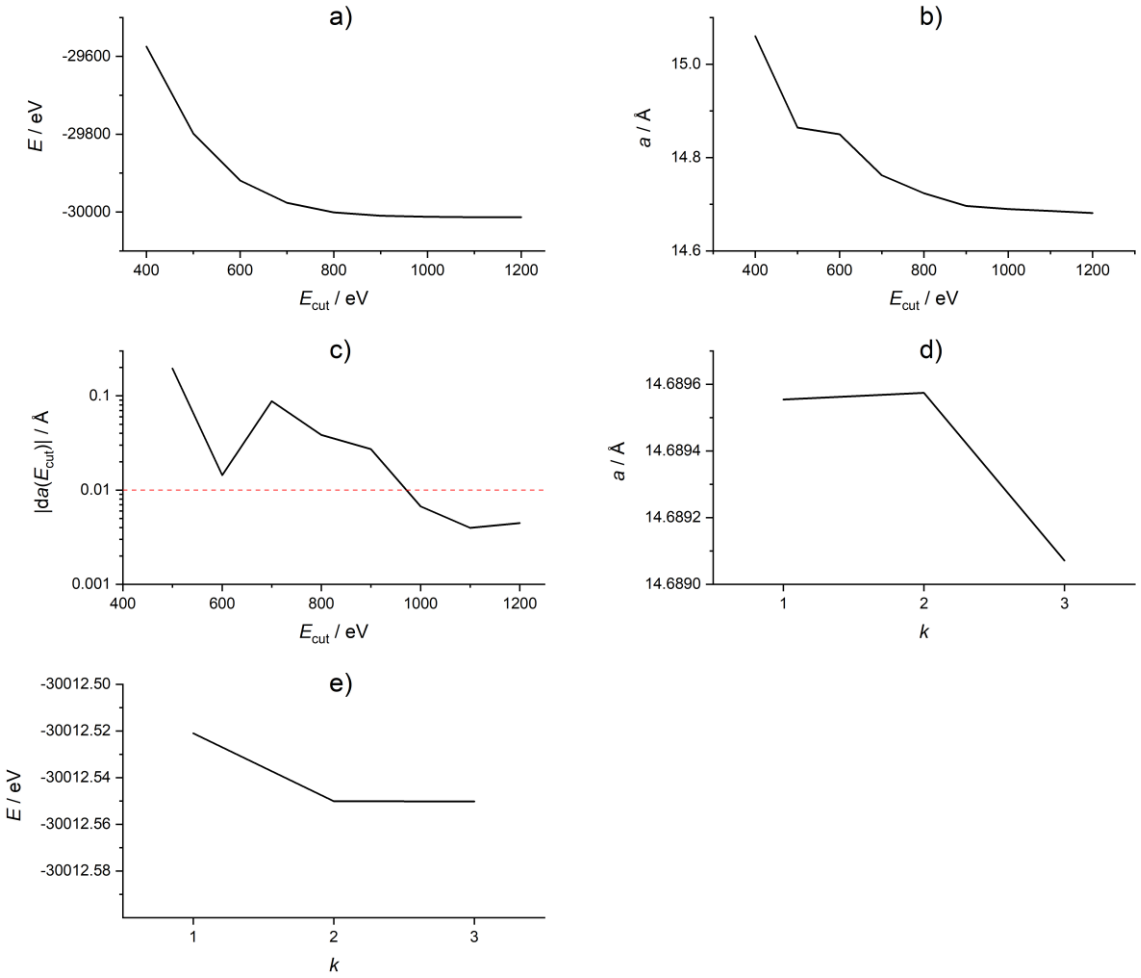

Figure S7. UiO-66: Convergence of a) total energy, b) lattice parameter *a*, c) lattice parameter *a* (derivation), d) *k* points (energy) and e) *k* points (lattice).

UiO-66-F

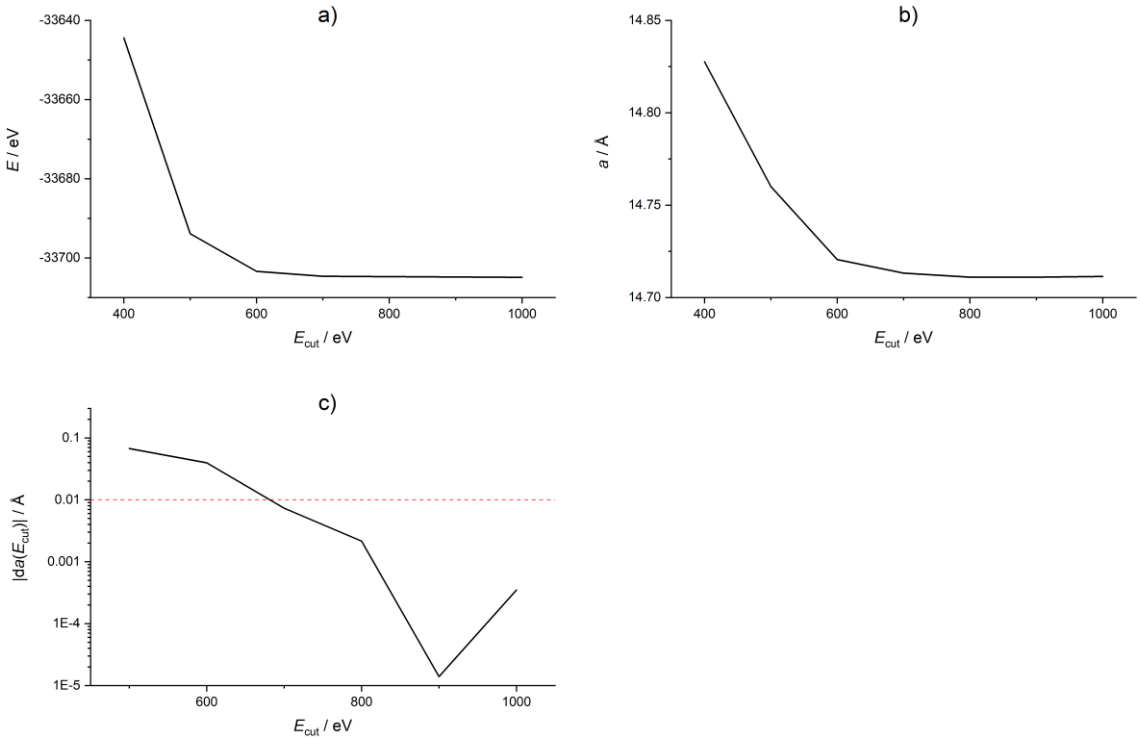

Figure S8. UiO-66-F: Convergence of a) total energy, b) lattice parameter *a* and c) lattice parameter *a* (derivation).

UiO-66-Cl

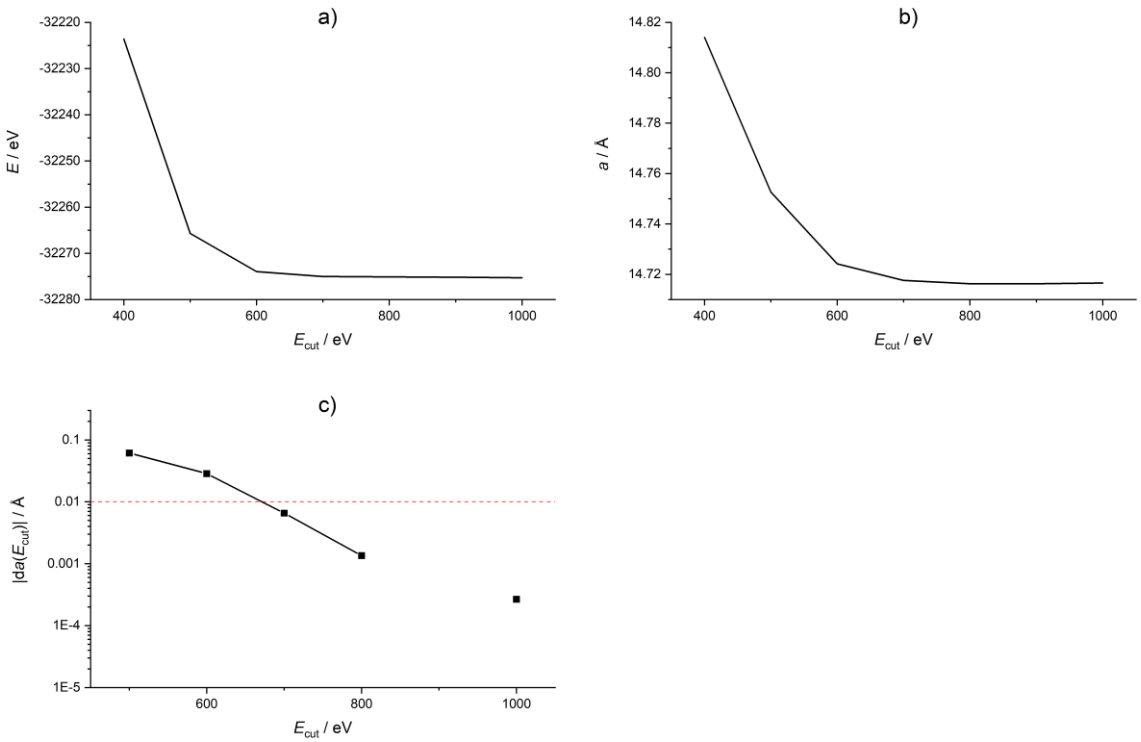

Figure S9. UiO-66-Cl: Convergence of a) total energy, b) lattice parameter *a* and c) lattice parameter *a* (derivation), derivation at 900 eV is 0 and not shown.

UiO-66-Br

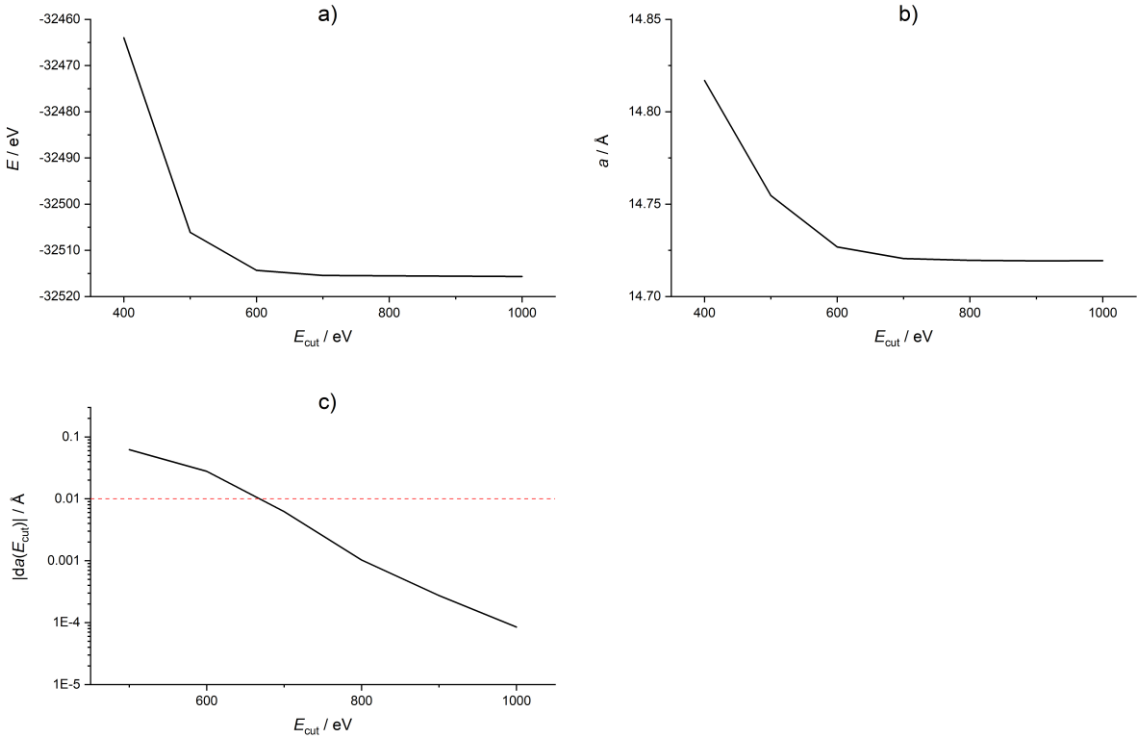

Figure S10. UiO-66-Br: Convergence of a) total energy, b) lattice parameter *a* and c) lattice parameter *a* (derivation).

UiO-66-I

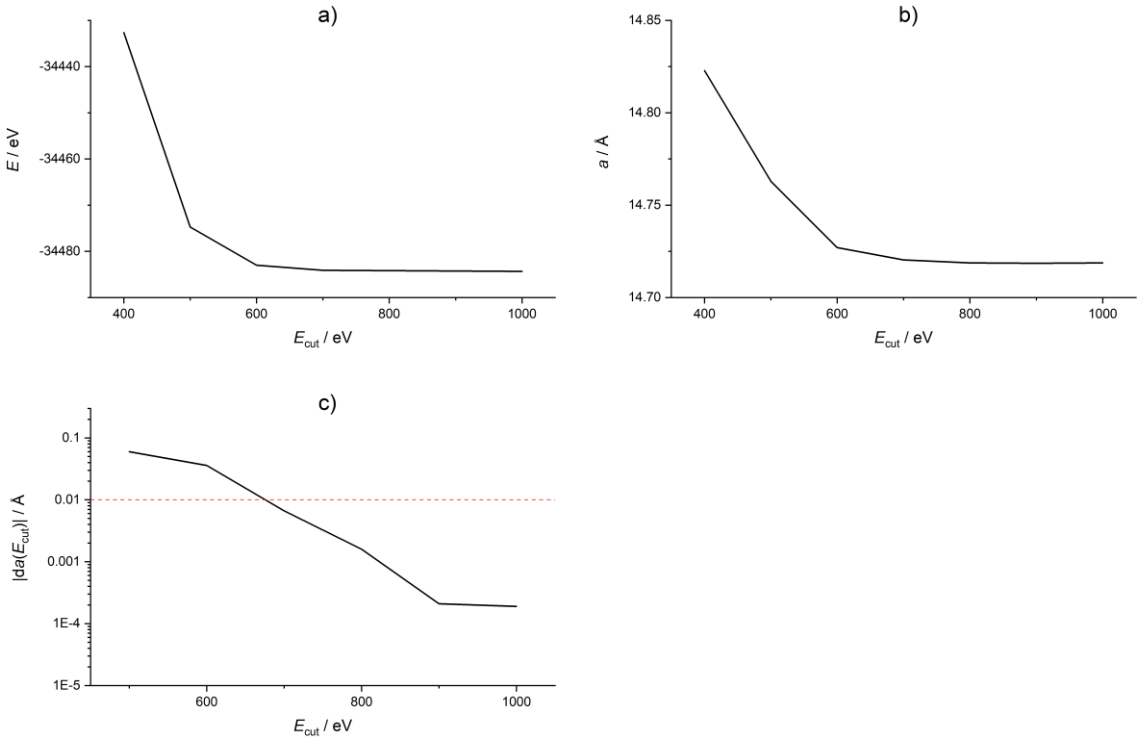

Figure S11. UiO-66-I: Convergence of a) total energy, b) lattice parameter *a* and c) lattice parameter *a* (derivation).

UiO-66-I_2

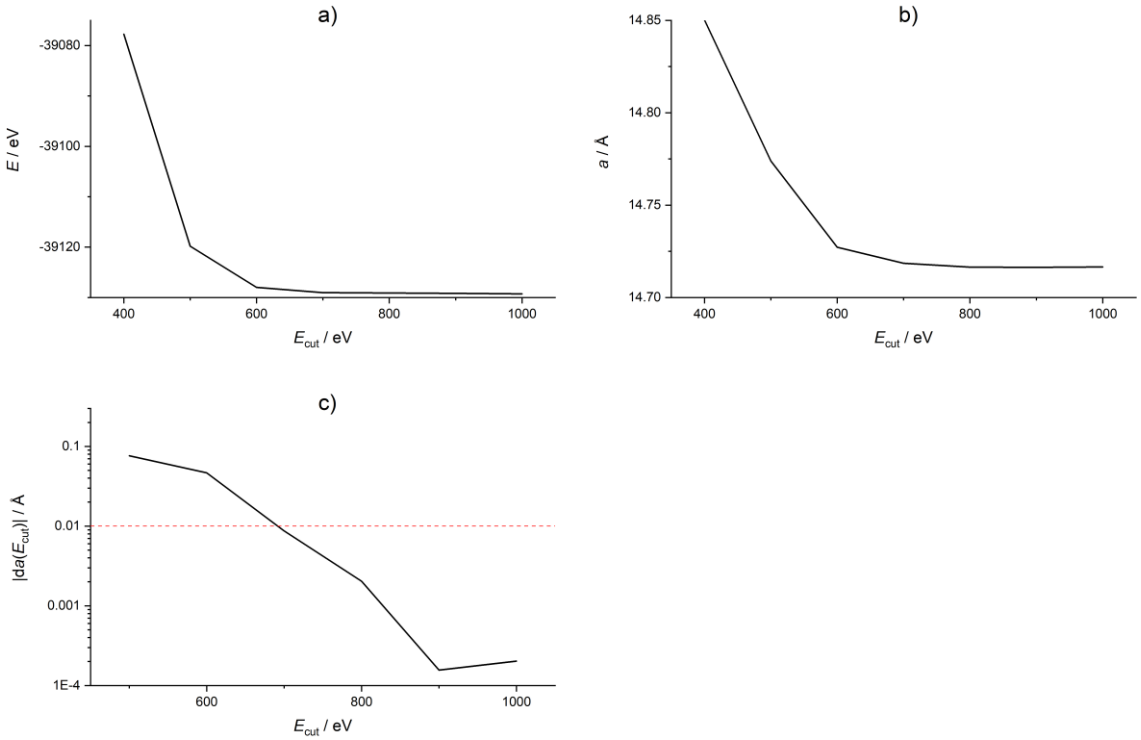

Figure S12. UiO-66-I_2: Convergence of a) total energy, b) lattice parameter *a* and c) lattice parameter *a* (derivation).

Section 3 XC functional benchmark

UiO-66

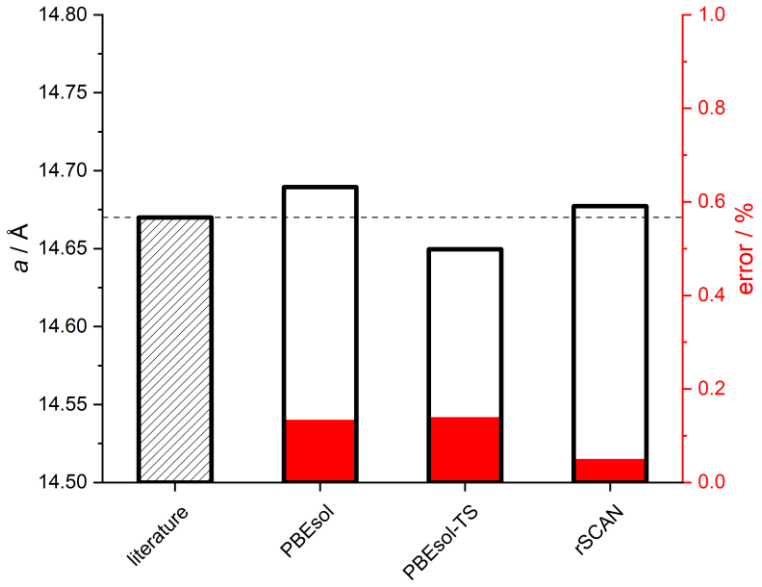

Figure S13. UiO-66: XC functional benchmark (absolute value black with relative error in red).

UiO-66-F

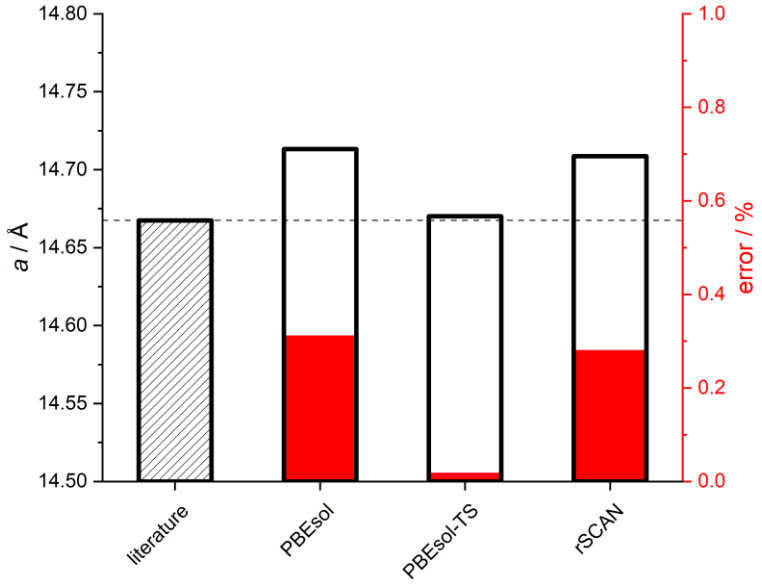

Figure S14. UiO-66-F: XC functional benchmark (absolute value black with relative error in red).

UiO-66-Cl

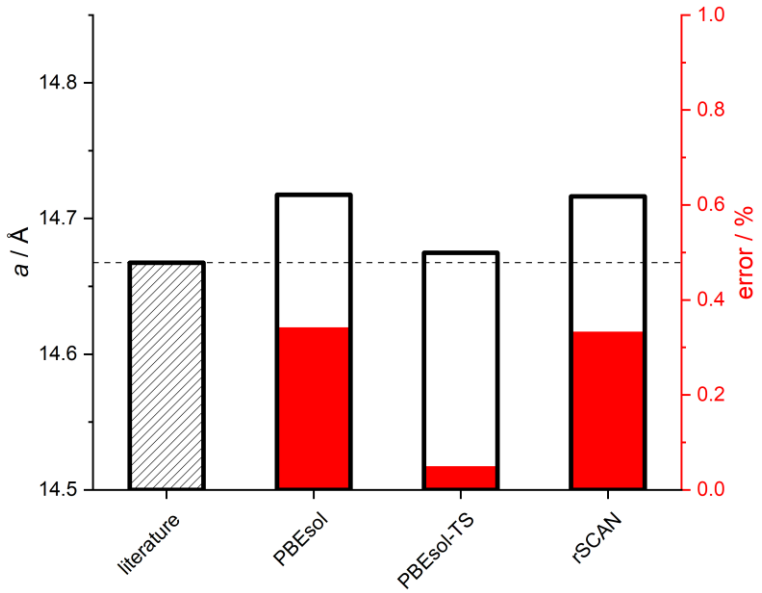

Figure S15. UiO-66-Cl: XC functional benchmark (absolute value black with relative error in red).

UiO-66-Br

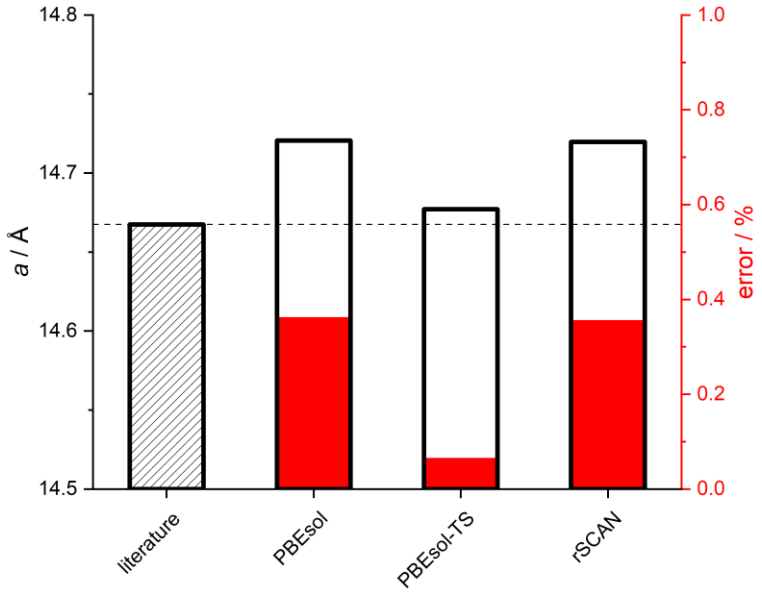

Figure S16. UiO-66-Br: XC functional benchmark (absolute value black with relative error in red).

UiO-66-I

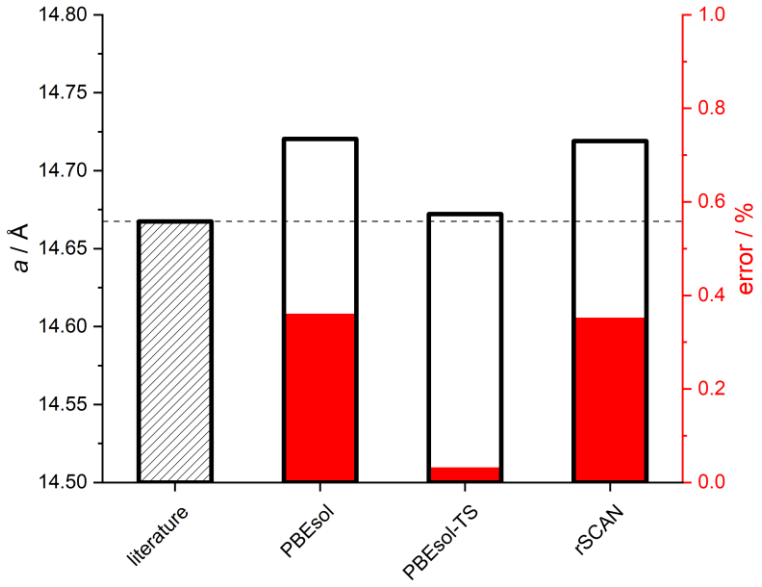

Figure S17. UiO-66-I: XC functional benchmark (absolute value black with relative error in red).

UiO-66-I_2

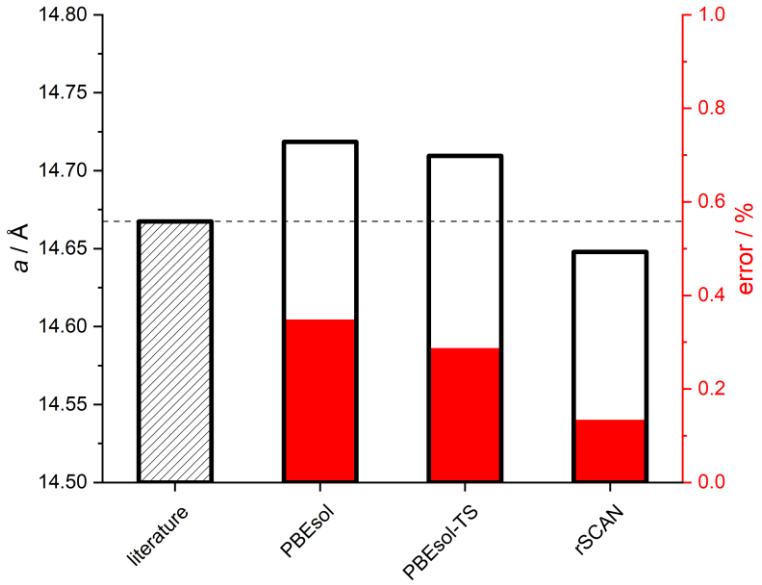

Figure S18. UiO-66-I_2: XC functional benchmark (absolute value black with relative error in red).

Section 4 Details of the DFT models

Table S1. Details of the DFT study and generated structural models of halogenated UiO-66 derivatives: space group, plane-wave kinetic energy cutoff, exchange-correlation functional, lattice parameter of the optimized primitive cell compared with the experimental UiO-66 value.

MOF	Space group	E_{cut} / eV	XC functional	*a* / Å	Deviation / %
UiO-66 (exp.)[3]	*F*-43*m*			14.668	
UiO-66	*F*-43*m*	1000	rSCAN	14.677	0.050
UiO-66-F	*R*3	700	PBEsol-TS	14.670	0.018
UiO-66-Cl	*R*3	700	PBEsol-TS	14.675	0.049
UiO-66-Br	*R*3	700	PBEsol-TS	14.677	0.065
UiO-66-I	*R*3	700	PBEsol-TS	14.672	0.032
UiO-66-I_2	*R*3	700	rSCAN	14.648	0.133

Section 5 Band structures

Table S2. Comparison of calculated and experimental band gaps.

MOF	sim. / eV	exp. / eV
UiO-66	4.25	4.05
UiO-66-F	3.96	4.02
UiO-66-Cl	3.76	3.91
UiO-66-Br	3.71	3.84
UiO-66-I	3.16	3.64
UiO-66-I_2	2.89	3.31

UiO-66

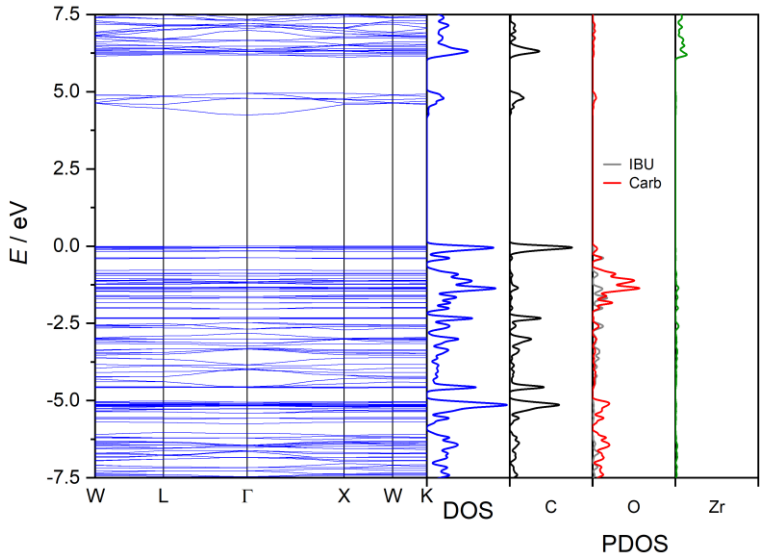

Figure S19. UiO-66 band structure with DOS and PDOS.

UiO-66-F

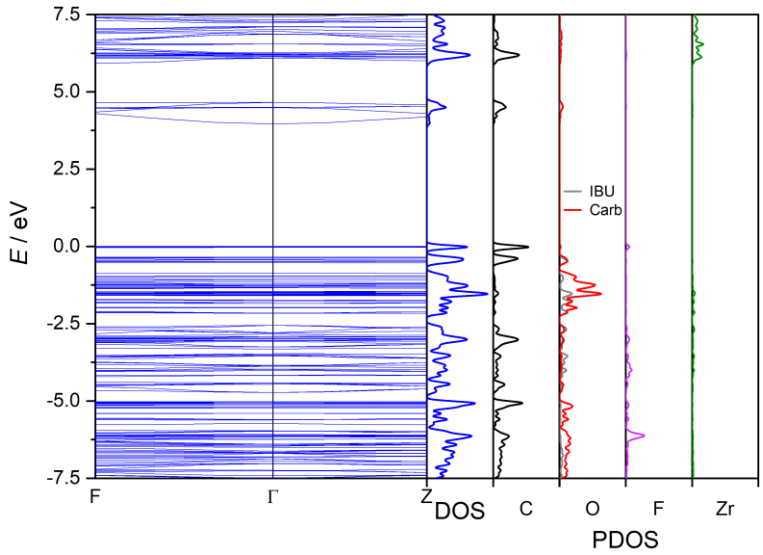

Figure S20. UiO-66-F band structure with DOS and PDOS.

UiO-66-Cl

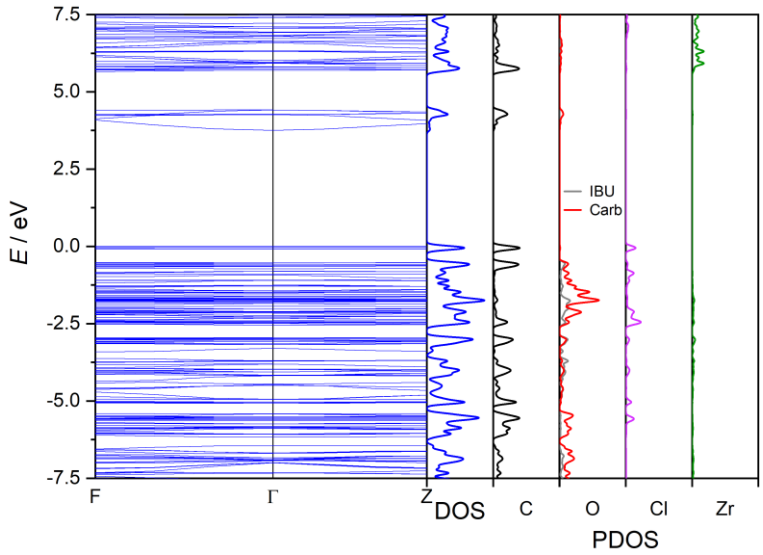

Figure S21. UiO-66-Cl band structure with DOS and PDOS.

UiO-66-Br

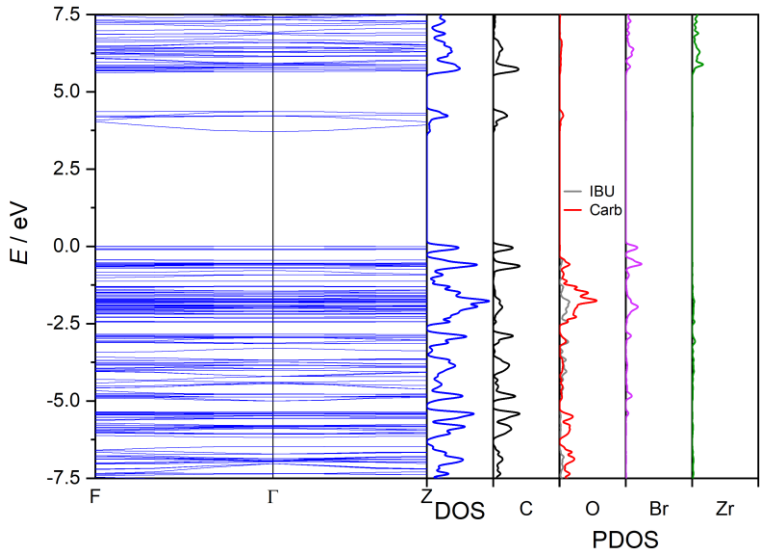

Figure S22. UiO-66-Br band structure with DOS and PDOS.

UiO-66-I

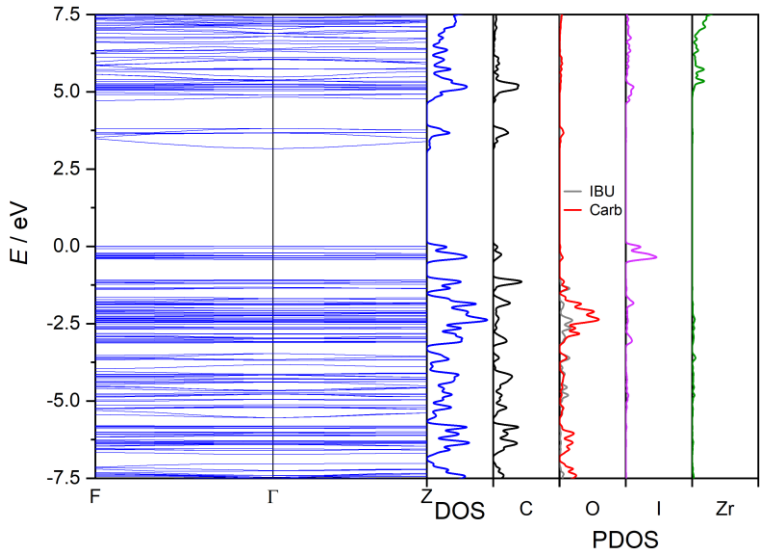

Figure S23. UiO-66-I band structure with DOS and PDOS.

UiO-66-I₂

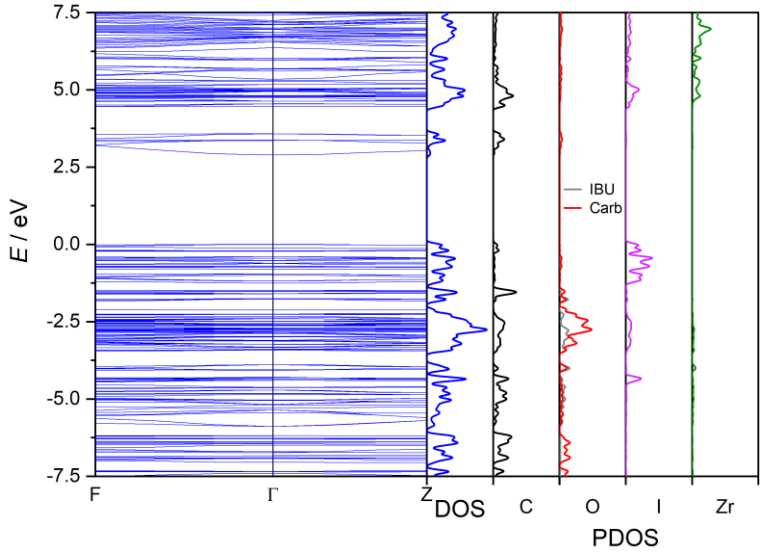

Figure S24. UiO-66-I₂ band structure with DOS and PDOS.

Section 6 Refractive Index

Table S3. Comparison of calculated refractive indices at 589 nm.

MOF	n_{589}
UiO-66	1.373
UiO-66-F	1.375
UiO-66-Cl	1.416
UiO-66-Br	1.433
UiO-66-I	1.488
UiO-66-I_2	1.585

References

[1] G. C. Shearer, S. Chavan, J. Ethiraj, J. G. Vitillo, S. Svelle, U. Olsbye, C. Lamberti, S. Bordiga, K. P. Lillerud, *Chem. Mater.* **2014**, *26*, 4068-4071.

[2] Q. Zhou, T. M. Swager, *J. Am. Chem. Soc.* **1995**, *117*, 12593.

[3] S. Øien, D. Wragg, H. Reinsch, S. Svelle, S. Bordiga, C. Lamberti, K. P. Lillerud, *Cryst. Growth Des.* **2014**, *14*, 5370.